

# Branched flow of intense laser light in porous media

K. Jiang,<sup>1,2</sup> T. W. Huang,<sup>1,\*</sup> C. N. Wu,<sup>3</sup> M. Y. Yu,<sup>1</sup> A. Pukhov,<sup>4</sup> C. T. Zhou,<sup>1,2,†</sup> and S. C. Ruan<sup>1,2</sup>

<sup>1</sup>Shenzhen Key Laboratory of Ultraintense Laser and Advanced Material Technology,  
Center for Advanced Material Diagnostic Technology, and College of Engineering Physics,  
Shenzhen Technology University, Shenzhen 518118, People's Republic of China

<sup>2</sup>College of Applied Sciences, Shenzhen University, Shenzhen 518060, People's Republic of China

<sup>3</sup>Graduate School, China Academy of Engineering Physics, Beijing 100088, People's Republic of China

<sup>4</sup>Institut für Theoretische Physik I, Heinrich-Heine-Universität Düsseldorf, 40225 Düsseldorf, Germany  
(Dated: September 30, 2021)

Branched flow is an interesting phenomenon that can occur in diverse systems. It is usually considered a linear phenomenon in that the flow does not alter the medium properties. Branched flow of laser light has recently been discovered. This provides an opportunity for investigating whether nonlinear branched flow can also occur. Here we found by two-dimensional particle-in-cell simulations that intense laser light propagating in a porous medium can indeed form light branches. In particular, dynamic ionization induced by the laser can enhance the density variations along the laser path and thus the light branching. However, too-intense lasers can suppress branching by smoothing the electron density. The branching properties and the location of the first branching point agrees well with an analysis based on a Schrödinger-like equation for the laser electric field. Branched flow of intense light in plasma opens up a new realm of intense laser-matter interaction, which would arouse broad interest in many research areas.

Waves propagating in a randomly uneven or clumpy medium with correlation length larger than the wavelength  $\lambda$  can form filaments in a treebranch-like manner [1–4]. This phenomenon, known as branched flow, has been observed in diverse systems and at many length scales [5–20]. For example, instead of smoothly diffusing or spreading, an electron beam passing through two-dimensional electron gases can form branching strands that become successively narrower [6–10], giant freak ocean waves are attributed to the random unevenness on the ocean floor [11–14], and branching of microwave radiation emitted by pulsars is suggested to be attributed to the interstellar dust clouds [15–17]. Recently, branched flow of laser light has been found on thin soap films [21]. The light branching is attributed to variations of the film's refractivity, which bends and bundles the light rays at favorable locations and form caustics [21]. Despite its complexity, branched flow is usually a linear phenomenon [22] and the distance  $d_0$  from the source to the first branching point follows the scaling  $d_0 \sim l_c v_0^{-2/3}$  [1, 18, 23], where  $l_c$  is the correlation length of the medium's unevenness, and  $v_0$  is a strength parameter (to be defined later).

With laser intensity  $I\lambda_{\mu\text{m}}^2 \gtrsim 10^{14}$  W/cm<sup>2</sup>, where  $\lambda_{\mu\text{m}}$  is the wavelength in units of  $\mu\text{m}$ , the atomic Coulomb barrier is suppressed by the strong laser electric field, the electrons are set free and the affected medium is ionized into a plasma [24], whose optical properties then become dominated by the electron dynamics. Moreover, at higher laser intensities  $I\lambda_{\mu\text{m}}^2 > 1.37 \times 10^{18}$  W/cm<sup>2</sup>, namely, the laser intensity is above the relativistic threshold, in addition to dynamic ionization, the laser ponderomotive force acting on the plasma can lead to highly disordered variations in the density and thus the local refractivity,

thereby affecting the laser propagation [25]. A timely and critical question is that whether light branching still survives in such intense laser-matter interactions involving with complex nonlinear effects, which however remains unclear.

In this Letter, we present the first investigation on nonlinear branched flow of intense light in laser-matter interaction. Particle-in-cell (PIC) simulations show that branched flow of the laser light can still occur at moderate laser intensities ( $I\lambda_{\mu\text{m}}^2 \sim 10^{15} - 10^{19}$  W/cm<sup>2</sup>) in an uneven medium, however, it becomes critically dependent on the laser intensity, which is distinct from the linear ones. In particular, the ionization induced by the strong laser electric field raises the unevenness of the refractivity along the laser path, and enhances the branching. However, too-intense laser light ( $I\lambda_{\mu\text{m}}^2 > 10^{19}$  W/cm<sup>2</sup>) can suppress light branching by smoothing the unevenness and thus the local refractivity of the plasma. An analysis of the branching process and the resulting properties that agree well with the simulation results is also given.

It may be useful to first discuss the physics of laser light branching in intense laser-matter interaction. Propagation of laser in a medium with uneven density distribution can be described by the two-dimensional (2D) Helmholtz equation [21]

$$-\nabla^2 \mathbf{E} + k_0^2(\bar{\eta}^2 - \eta_{\text{eff}}^2) \mathbf{E} = k_0^2 \bar{\eta}^2 \mathbf{E}, \quad (1)$$

where  $\mathbf{E}(x, y)$  is the laser electric field,  $k_0 = 2\pi/\lambda_0$  is the wave number in vacuum,  $\eta_{\text{eff}}(x, y)$  is the effective refractive index, and  $\bar{\eta}^2 = \langle \eta_{\text{eff}}^2 \rangle$  is its mean-square value. Here,  $\langle \dots \rangle = \frac{1}{S} \int \dots dS$ , where  $dS$  is the surface element and the integration is over the laser spot area.

Upon irradiation, the medium is ionized by the strong laser electric field into a plasma. The resulting plasma

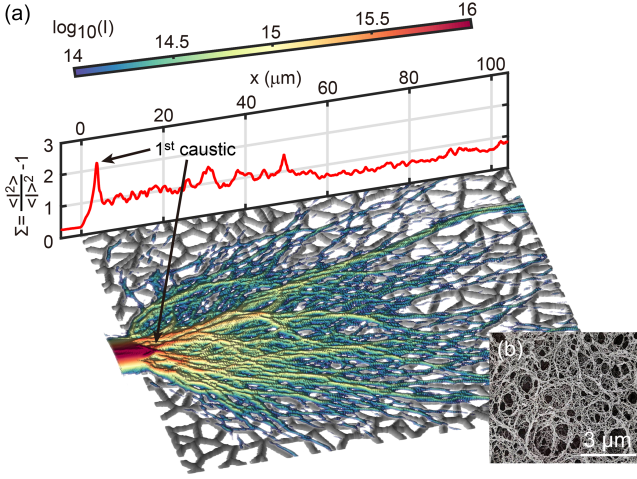


FIG. 1. (a) Flow branching as an intense laser propagates through a porous foam along the  $x$  direction. The (logarithmic) color bar is for the laser intensity in  $\text{W}/\text{cm}^2$  at  $t = 534$  fs. The foam structure is shown below in gray color. The red curve is for the spatial evolution of the corresponding scintillation index  $\Sigma = (\langle I^2 \rangle / \langle I \rangle^2) - 1$  of the laser light. The arrows mark the first caustic, or branching point. (b) Scanning electron micrograph of  $\text{SiO}_2$  foam fabricated with a sol-gel process.

refractivity can be written as  $\eta_{\text{eff}} = \sqrt{1 - n_e(I)/\gamma n_c}$ , where  $n_c = m_e \omega^2 \epsilon_0 / e^2$  is the critical plasma density,  $\gamma = \sqrt{1 + a_0^2/2}$  and  $\gamma = \sqrt{1 + a_0^2}$  for linear and circular polarization, respectively,  $a_0 = e|\mathbf{E}|/m_e \omega c$  is the normalized laser electric field,  $m_e$  and  $-e$  are the electron rest mass and charge,  $\omega$  is the laser frequency,  $\epsilon_0$  is the vacuum permittivity, and  $c$  is the speed of light in vacuum. Note that the electron number density  $n_e$  is a function of the instantaneous laser intensity  $I$  since the electrons are produced by photoionization.

Substituting  $\eta_{\text{eff}}$  into Eq. (1), one obtains

$$-\nabla^2 \mathbf{E} = \frac{k_0^2}{n_c} \left[ n_c - \left( \frac{n_e(I)}{\gamma} - \delta(I) \right) \right] \mathbf{E}, \quad (2)$$

where  $\delta(I) = \langle n_e(I)/\gamma \rangle - n_e(I)/\gamma$  describes the unevenness of the random medium. Eq. (1) is analogous to the time-independent nonlinear Schrödinger equation  $\frac{\hbar^2}{2m_e} \nabla^2 \psi + U\psi = E\psi$  describing branch formation of electron beam passing through electron gases [6–10]. The potential energy  $U$  is analogous to our  $V = -k_0^2 \delta(I)/n_c$ . It has been shown [1, 18, 23] that for  $U \ll E$ , due to the positive correlation between the branched flow and  $U$ , branch pattern development depends directly on the initial unevenness of the medium. However, in our case the nonlinear term  $n_{e,\text{eff}} = [n_e(I)/\gamma - \delta(I)]$  in Eq. (2) includes the effects of both the dynamic ionization and the interaction between the laser and the electrons through the ponderomotive and relativistic effects, which also affect the laser propagation.

If  $I \lambda_{\mu\text{m}}^2 \ll 1.37 \times 10^{18} \text{ W}/\text{cm}^2$ , one has  $\gamma \sim 1$

and relativistic effects are negligible. In this case  $n_{e,\text{eff}} = [2n_e(I) - \langle n_e(I) \rangle]$ , and both  $\langle n_{e,\text{eff}}^2 \rangle / \langle n_{e,\text{eff}} \rangle^2$  and  $\langle \delta(I)^2 \rangle / \langle \delta(I) \rangle^2$  would increase with  $I$  due to an increased ionization rate. Thus the dynamic ionization could enhance the unevenness of the refractivity variations along the laser paths, and thus affect the branch formation. However, for  $I \lambda_{\mu\text{m}}^2 > 1.37 \times 10^{18} \text{ W}/\text{cm}^2$ , most of the electrons on the outer shells of the atoms are freed and they can be accelerated to light speed by the laser field in a single cycle. In this case, further ionization becomes marginal and the relativistic effects become significant. If we assume  $n_e$  is time-independent, and ignore the smoothing effect of both laser ponderomotive force and plasma thermal expansion at an initial stage, we have  $n_{e,\text{eff}} = n_e (2/\gamma - \langle 1/\gamma \rangle)$ , where  $n_e$  almost saturates. In this case,  $\langle n_{e,\text{eff}}^2 \rangle / \langle n_{e,\text{eff}} \rangle^2$  and  $\langle \delta(I)^2 \rangle / \langle \delta(I) \rangle^2$  decrease with increase of  $I$  due to the relativistic effects, indicating that relativistic transparency [26] smooths the refractivity variations. As a result, it can be theoretically predicted that in the interaction light branching first increases with  $I$ , then saturates at around the relativistic threshold, and is suppressed if  $I$  becomes too large.

We have carried out 2D PIC simulations of the laser ionization and branching process using the EPOCH code [27]. As illustrated in Fig. 1(a), the initial porous medium has a Voronoi structure of  $\text{SiO}_2$  [28] and is located in  $0 < x < 100 \mu\text{m}$  and  $-50 \mu\text{m} < y < 50 \mu\text{m}$ . The number densities of Si and O atoms in the fibers are  $0.05n_c$  and  $0.1n_c$ , respectively, with filling factor 24%, corresponding to  $\text{SiO}_2$  foam of  $2 \text{ mg}/\text{cm}^3$  fabricated by a sol-gel process, and shown in Fig. 1(b). The average length scale of the pores of  $l_c = 3.4 \mu\text{m}$  is obtained from auto-correlation function [29]. A circularly-polarized intense Gaussian laser of central wavelength  $\lambda = 800 \text{ nm}$ , peak intensity  $I_0 = 10^{16} \text{ W}/\text{cm}^2$ , and waist radius  $r_0 = 4.8 \mu\text{m}$  incidents normally from the left boundary at  $x = -5 \mu\text{m}$ . For simplicity, the laser is of flat-top time profile. The simulation box is of size  $-5 \mu\text{m} < x < 105 \mu\text{m}$  and  $-55 \mu\text{m} < y < 55 \mu\text{m}$ , with  $1100 \times 1000$  grid cells and 60 macroparticles per cell for both Si and O atoms. Open lateral boundaries are used.

Fig. 1(a) for the distribution of the laser intensity at  $t = 534$  fs clearly shows the light branching. The laser pulse breaks up into several filaments after the first caustic at around  $x = 3.7 \mu\text{m}$ . As they propagate, the filaments further break up into narrower and weaker ones in a cascade manner. Such bifurcation of intense lasers does not seem to have been reported before. A useful quantity to characterize the branch pattern is the scintillation index  $\Sigma = (\langle I^2 \rangle / \langle I \rangle^2) - 1$ , which measures the relative strength of intensity fluctuations [19]. Here the averages are taken over the laser spot area. We see that  $\Sigma$  increases from 0.25 at the foam front surface to 2.20 at  $x = 3.7 \mu\text{m}$ . The nonzero

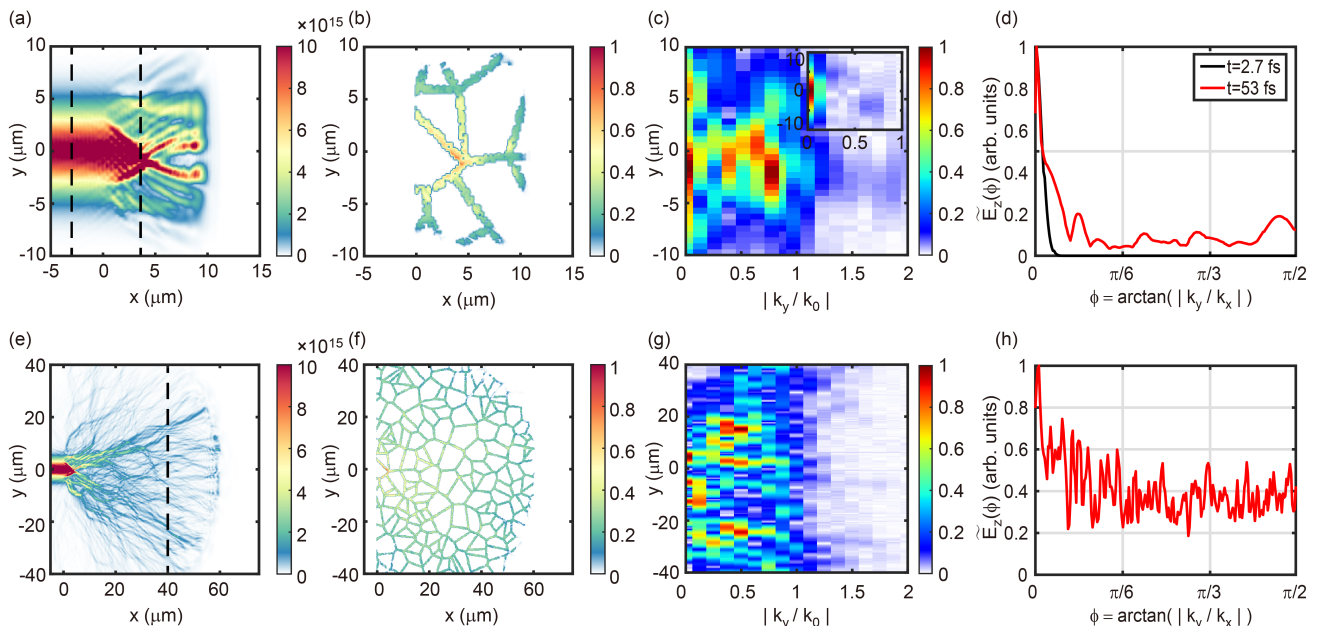


FIG. 2. Simulation results at  $t = 53$  fs of the (a) laser intensity (in  $\text{W}/\text{cm}^2$ ), (b) electron number density (in  $n_c$ ), and (c) lateral wavenumber  $|k_y/k_0|$  at  $x = 3.7 \mu\text{m}$  of the laser electric field  $E_z$ . The inset in (c) shows  $|k_y/k_0|$  at  $x = -3 \mu\text{m}$ . (d) The strength  $\tilde{E}_z(\phi)$  (see text for definition) versus the spreading angle  $\phi$ . (e)-(h) Same as (a)-(d), but at  $t = 240$  fs.

initial value here is due to the Gaussian profile. The dependence of  $\Sigma$  on  $x$  agrees well with the branch pattern of the laser intensity. Since optical turbulence is defined by  $\Sigma > 1$  [30], so that here the laser pulse evolves from Gaussian to strongly fluctuated within only  $3.7 \mu\text{m}$ , much shorter than that of typical filamentation instabilities [31–36]. It should be emphasized that the laser branching observed here is fundamentally different from laser filamentation in plasmas, where a sufficiently intense laser can break up into narrow parallel filaments, usually without further bifurcation as they propagate. It is noted that similar branch formation can also be observed in simulations with various foam structures (see Supplementary Materials).

We now consider in more detail the branching process. Upon irradiation, the fibers of the foam are ionized into a fibrous plasma (before significant thermal expansion can take place). At the laser intensity  $I = 1 \times 10^{16} \text{ W}/\text{cm}^2$ , tunnel ionization of both the Si and O atoms to the +4 state can occur [24]. For our simulation parameters, the number density  $n_e$  of the fiber electrons around the laser axis should thus be  $0.6n_c$ . Fig. 2(b) shows that the  $n_e$  distribution agrees with our estimate (for more details on the dynamic ionization, see Supplementary Information). The uneven plasma starts to locally focus the laser light to higher intensity, leading to even higher  $n_e$  at the nodes. Such a positive feedback stops when  $n_e > n_c$ , at around  $x = 3.7 \mu\text{m}$ . That is, locally the foam plasma becomes opaque to the laser light, which is then diverted into directions where the plasma density is below critical and low, as can be seen in Fig. 2(a). The sideways scattering

of the laser light at the nodes is demonstrated by the appearance of the lateral wavenumber  $k_y$  in Fig. 2(c) for the  $(|k_y|, y)$  phase space. In particular, at  $y = -1.8 \mu\text{m}$ , the dominant lateral wave numbers are  $|k_y| = 0, 0.38k_0$  and  $0.75k_0$ , whereas  $k_y$  is practically null at  $x = -3 \mu\text{m}$  (outside the fibrous plasma, see the inset). It may be of interest to note that such a multivalued  $k_y$  distribution corresponds to foldings in the Lagrangian manifold  $\mathcal{L}$ , and is a typical feature of caustics [37–39]. Due to the foam structure, the process of focusing, caustics formation, and branching of the laser light tend to repeat, resulting in branched flow as shown in Fig. 1 and Fig. 2(e). With the development of optical turbulence, the  $(|k_y|, y)$  phase space becomes more chaotic over time, as can be seen in Fig. 2(g).

The evolution of the  $(|k_y|, y)$  phase space discussed above reflects branching of the laser light in the physical space. To further characterize the branching, we consider the angular dependence of the laser electric field in the Fourier space, defined by  $\tilde{E}_z(\phi) = |\int e^{-ik_0x \cos \phi} e^{-ik_0y \sin \phi} E_z(\phi) dx dy|$ , where  $\phi = \arctan(|k_y/k_x|)$ . Here,  $E_z$  is used instead of  $E_y$  to exclude the non-oscillating self-generated fields. As shown in Fig. 2(d), the dependence of  $\tilde{E}_z(\phi)$  on  $\phi$  at  $t = 2.7$  and  $53$  fs is quite similar for  $\phi < \pi/63$ , indicating that most of the laser energy still flows in the  $x$  direction. Even at  $t = 53$  fs, only a small fraction of the laser light is side scattered at the overdense nodes. However, we can see in Fig. 2(h) that at  $t = 240$  fs, as a result of many successive branchings in the foam structure, the light-filament distribution becomes rather isotropic

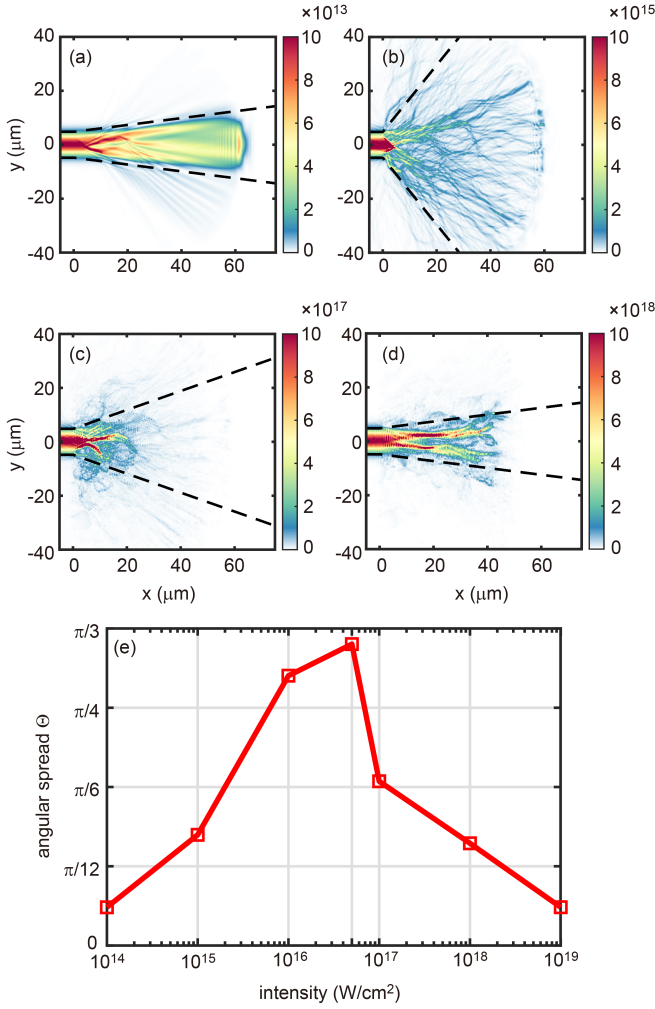


FIG. 3. Light intensity patterns at  $t = 240$  fs for input laser intensities (a)  $I_0 = 10^{14}$  W/cm<sup>2</sup>, (b)  $I_0 = 10^{16}$  W/cm<sup>2</sup>, (c)  $I_0 = 10^{18}$  W/cm<sup>2</sup>, and (d)  $I_0 = 10^{19}$  W/cm<sup>2</sup>. The black dashed lines mark the spread angles of the light branches. (e) Spread angle  $\Theta$  (in radians) of the branches versus the initial laser intensity.

within a large spread angle  $\phi = \pi/60 \sim \pi/2$ .

The boundaries of the spread angle  $\Theta$  of the light branches in the foam can be defined as that when  $\bar{E}_z$  drops to 1/4 of its maximum. We find  $\Theta = 2\pi/7$  for  $I = 1 \times 10^{16}$  W/cm<sup>2</sup>. This is 8 times larger than that associated with the Rayleigh length for laser propagating in vacuum, namely  $\Theta_{\text{Rayleigh}} \simeq 2r_0/z_R \simeq \pi/30$ , where  $z_R = \pi r_0^2/\lambda$  is the Rayleigh length. Figures 3(a)-(d) show the branch patterns for different laser intensities. One can clearly see that  $\Theta$  increases with  $I_0$  until  $I_0 \lesssim 10^{18}$  W/cm<sup>2</sup>, then it again becomes that of the original laser. This is in good agreement with our theoretical discussion above: branched flow should be strongest when the laser intensity approaches the relativistic threshold  $1.37 \times 10^{18}$  W/cm<sup>2</sup>, and should decrease after that. In fact, one can clearly see in (d) that relativistic transparency as well

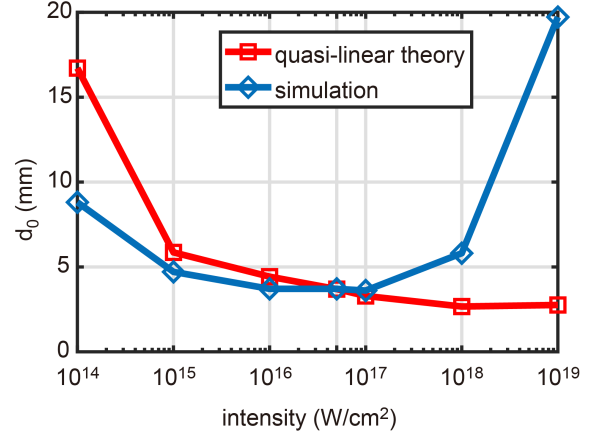


FIG. 4. The distance from the source to the first branching point  $d_0$  ( $\mu\text{m}$ ) for different laser intensities at  $t = 240$  fs. The red and blue curves are results from quasi-linear scaling and simulations, respectively.

as self-focusing of the laser are taking place, which can be expected at that laser intensity [31, 32]. Figure 3(e) shows the dependence of the spread angle  $\Theta$  on the initial laser intensity. One sees that spread of the branches is widest in the region of  $10^{16} - 10^{17}$  W/cm<sup>2</sup>. Such deviation from the theoretical prediction results from the fact that the plasma fibers can focus the laser light to filaments of higher intensity (as can be deduced from Figs. 2(a) and (b)), thus the initial intensity for the strongest branched flow shifts down below  $1.37 \times 10^{18}$  W/cm<sup>2</sup>.

As mentioned, a convenient parameter for characterizing flow-branching is the distance  $d_0$  from the boundary (where the flow enters) of the porous medium to the first branching point. In the linear case, the flow has no influence on the medium, and a universal scaling law for  $d_0$  is  $d_0 \sim l_c v_0^{-2/3}$  [1, 18, 23], where the potential strength  $v_0$  is defined as the ratio of the standard deviation of the potential  $U$  and the energy  $E$  in the corresponding. For intense lasers, according to Eq. (1), the optical analogy of potential strength corresponds to  $v_0 = \sqrt{\langle(\bar{\eta}^2 - \eta_{\text{eff}}^2)^2\rangle}/2\bar{\eta}^2 = \sqrt{\langle(n_e(I)/\gamma - \langle n_e(I)/\gamma \rangle)^2\rangle}/2(n_c - \langle n_e(I)/\gamma \rangle)}$ . Recall that  $\delta(I) = \langle n_e(I)/\gamma \rangle - n_e(I)/\gamma$ , so that before significant plasma expansion can take place, i.e.,  $l_c$  remains constant,

$$d_0 \propto l_c \langle \delta(I)^2 \rangle^{-1/3} \left\langle n_c - \frac{n_e(I)}{\gamma} \right\rangle^{2/3}. \quad (3)$$

Note that the laser intensity appears in the scaling, which is due to the nonlinear effects of dynamic ionization and relativistic transparency. We see that  $d_0$  decreases with increase of the medium unevenness given by  $\langle \delta(I)^2 \rangle$ , and increases with  $\langle n_c - n_e(I)/\gamma \rangle$ , indicating that the higher the effective plasma density, the earlier branching occurs. Such quasi-linear scaling agrees well with that from the

simulations in the region of  $10^{15} \text{ W/cm}^2 < I_0 < 10^{18} \text{ W/cm}^2$  for strong branched flow, as shown in Fig. 4. However, for  $I_0 > 10^{18} \text{ W/cm}^2$ , the theoretical scaling is largely deviated from the simulations. In this case,  $d_0$  from the quasi-linear theory presents a much slower increase with  $I_0$ , as compared with that from simulations. This can be attributed to the fact that self-focusing of the laser and thermal expansion of the fiber electrons, which are not included in our theory but are self-consistently included in the simulations, can greatly reduce and smooth the affected electron density. The persistence of correlated structure of the porous foam can be roughly estimated as  $\tau = l_c/2c_s$ . Here  $c_s = \sqrt{ZT_e/m_i}$  is the ion sound velocity,  $Z$  is the ionization state, and  $T_e$  is the bulk electron temperature, which is typically  $a_0 m_e c^2$  [40]. At  $I = 10^{19} \text{ W/cm}^2$ , one obtains that the porous structure persists within only  $\tau \sim 300 \text{ fs}$ . Thus, in order to accurately predict the first branching point for relativistic lasers, the increase of  $l_c$  by thermal expansion must be taken into account. In addition, at  $I = 10^{20} \text{ W/cm}^2$ , the porous structure is washed out within only 160 fs (see Supplementary Information), thus light-branching is suppressed by strong self-focusing and plasma expansion.

In conclusion, we have shown that an intense laser propagating through foam targets can form complex light branches. Dynamic ionization can raise unevenness in the density, and thus enhance branch formation. However, relativistic effects of too-intense lasers can suppress branch formation by smoothing the electron density unevenness. Our work extends the existing studies of optical branching to the nonlinear regime. The results may be relevant to optical communications, nonlinear optics, strong field physics, as well as laser interaction with foam and/or turbulent plasma.

This work is supported by the National Key R&D Program of China (Grant No. 2016YFA0401100), the National Natural Science Foundation of China (Grants No. 12175154, No. 11875092, and No. 12005149), the Natural Science Foundation of Top Talent of SZTU (Grant No. 2019010801001 and 2019020801001). The EPOCH code is used under UK EPSRC contract(EP/G055165/1 and EP/G056803/1). We thank X. Luo from LFRC for providing the scanning electron micrograph of SiO<sub>2</sub> foam fabricated with a sol-gel process. K. J. would like to thank X. F. Shen, H. Peng, and T. Y. Long for useful discussions.

## REFERENCES

- † [zangtao@sztu.edu.cn](mailto:zangtao@sztu.edu.cn)
- [1] L. Kaplan, Statistics of branched flow in a weak correlated random potential. *Phys. Rev. Lett.* **89**, 184103 (2002).
  - [2] J. J. Metzger, R. Fleischmann, and T. Geisel, Universal statistics of branched flows. *Phys. Rev. Lett.* **105**, 020601 (2010).
  - [3] J. J. Metzger, R. Fleischmann, and T. Geisel, Statistics of extreme waves in random media. *Phys. Rev. Lett.* **112**, 203903 (2014).
  - [4] E. J. Heller, R. Fleischmann, T. Kramer, Branched flow. arXiv preprint: 1910.07086 (2019).
  - [5] S. Zapperi, P. Ray, H. E. Stanley, and A. Vespignani, First-order transition in the breakdown of disordered media, *Phys. Rev. Lett.* **78**, 1408 (1997).
  - [6] M. A. Topinka, B. J. LeRoy, R. M. Westervelt, S. E. J. Shaw, R. Fleischmann, E. J. Heller, K. D. Maranowski, and A. C. Gossard, Coherent branched flow in a two-dimensional electron gas. *Nature (London)* **410**, 183 (2001).
  - [7] K. E. Aidala, R. E. Parrott, T. Kramer, E. J. Heller, R. M. Westervelt, M. P. Hanson, and A. C. Gossard, Imaging magnetic focusing of coherent electron waves. *Nat. Phys.* **3**, 464 (2007).
  - [8] M. P. Jura, M. A. Topinka, L. Urban, A. Yazdani, H. Shtrikman, L. N. Pfeiffer, K. W. West, and D. Goldhaber-Gordon, Unexpected features of branched flow through high-mobility two-dimensional electron gases. *Nat. Phys.* **3**, 841 (2007).
  - [9] D. Maryenko, F. Ospald, K. von Klitzing, J. Smet, J. J. Metzger, R. Fleischmann, T. Geisel, and V. Umansky, How branching can change the conductance of ballistic semiconductor devices. *Phys. Rev. B* **85**, 195329 (2012).
  - [10] B. Liu and E. J. Heller, Stability of branched flow from a quantum point contact, *Phys. Rev. Lett.* **111**, 236804 (2013).
  - [11] M. V. Berry, Tsunami asymptotics. *New J. Phys.* **7**, 129 (2005).
  - [12] M. V. Berry, Focused tsunami waves. *Proc. Roy. Soc. A* **463**, 3055 (2007).
  - [13] U. Kanoglu, V. V. Titov, B. Aydin, C. Moore, T. S. Stefanakis, H. Q. Zhou, M. Spillane, and C. E. Synolakis, Focusing of long waves with finite crest over constant depth. *Proc. R. Soc. A* **469**, 20130015 (2013).
  - [14] H. Degueldre, J. J. Metzger, T. Geisel, and R. Fleischmann, Random focusing of tsunami waves, *Nat. Phys.* **12** 259 (2016).
  - [15] J. Cordes, A. Pidwerbetsky, and R. Lovelace, Refractive and diffractive scattering in the interstellar medium, *Astrophys. J.* **310** 737 (1986).
  - [16] A. Pidwerbetsky, Simulation and analysis of wave propagation through random media, Ph.D. thesis, Cornell University (1988).
  - [17] D. R. Stinebring, Scintillation Arcs: Probing Turbulence and Structure in the ISM. *Chin. J. Astron. Astrophys.* **6**, 204 (2006).
  - [18] S. Barkhofen, J. J. Metzger, R. Fleischmann, U. Kuhl, and H.-J. Stöckmann, Experimental Observation of a fundamental length scale of waves in random media, *Phys. Rev. Lett.* **111**, 183902 (2013).
  - [19] G. Green and R. Fleischmann, Branched flow and caustics in nonlinear waves, *New J. Phys.* **21**, 083020 (2019).
  - [20] N. J. Derr, D. C. Fronk, C. A. Weber, A. Mahadevan, C.

---

\* [huangtaiwu@sztu.edu.cn](mailto:huangtaiwu@sztu.edu.cn)

- H. Rycroft, and L. Mahadevan, Flow-driven branching in a frangible porous medium, *Phys. Rev. Lett.* **125**, 158002 (2020).
- [21] A. Patsyk, U. Sivan, M. Segev, and M. A. Bandres, Observation of branched flow of light, *Nature* **583**, 60 (2020).
- [22] A. Brandstöttera, A. Girschika, P. Ambichla, and S. Rottera, Shaping the branched flow of light through disordered media, *Proc. Natl. Acad. Sci.* **116**, 13260 (2019).
- [23] M. Mattheakis and G. P. Tsironis, Extreme waves and branching flows in optical media, *Quodons in Mica*. 425 (2015).
- [24] S. Augst, D. Strickland, D. D. Meyerhofer, S. L. Chin, and J. H. Eberly, Tunneling ionization of noble gases in a high-intensity laser field. *Phys. Rev. Lett.* **63**, 2212 (1989).
- [25] P. Gibbon. Short pulse laser interactions with matter: an introduction. (World Scientific, 2005).
- [26] S. Palaniyappan, B. M. Hegelich, H.-C. Wu, D. Jung, D. C. Gautier, L. Yin, B. J. Albright, R. P. Johnson, T. Shimada, S. Letzring, D. T. Offermann, J. Ren, C. K. Huang, R. Hörlein, B. Dromey, J. C. Fernandez, and R. C. Shah, Dynamics of relativistic transparency and optical shuttering in expanding overdense plasmas. *Nat. Phys.* **8**, 763 (2012).
- [27] T. D. Arber, K. Bennett, C. S. Brady, A. Lawrence-Douglas, M. G. Ramsay, N. J. Sircombe, P. Gillies, R. G. Evans, H. Schmitz, A. R. Bell, and C. P. Ridgers, Contemporary particle-in-cell approach to laser-plasma modelling. *Plasma Phys. Control. Fusion* **57**, 113001 (2015).
- [28] Y. Z. Song, Z. H. Wang, L. M. Zhao, and J. Luo, Dynamic crushing behavior of 3D closed-cell foams based on Voronoi random model. *Mater. Des.* **31**, 4281 (2010).
- [29] E. S. Gademawlam, M. M. Koura, T. M. A. Maksoud, I. M. Elewa, and H. H. Soliman, Roughness parameters. *J. Mater. Sci.* **123**, 133 (2002).
- [30] R. Z. Rao, Scintillation index of optical wave propagating in turbulent atmosphere. *Chin. Phys. B*, **18**, 581 (2009).
- [31] P. K. Shukla, N. N. Rao, M. Y. Yu and N. L. Tsintsadze, Relativistic nonlinear effects in plasmas, *Phys. Reports* **138**, 1-149 (1986)
- [32] G. Z. Sun, E. Ott, Y. C. Lee, and P. Guzdar, Self-focusing of short intense pulses in plasmas. *Phys. Fluids* **30**, 526 (1987);
- [33] A. B. Borisov, A. V. Borovskiy, O. B. Shiryaev, V. V. Korobkin, A. M. Prokhorov, J. C. Solem, T. S. Luk, K. Boyer, and C. K. Rhodes, Relativistic and charge-displacement self-channeling of intense ultrashort laser pulses in plasmas. *Phys. Rev. A* **45**, 5830 (1992);
- [34] A. B. Borisov, A. V. Borovskiy, A. Mcpherson, K. Boyer, and C. K. Rhodes, Stability analysis of relativistic and charge-displacement self-channelling of intense laser pulses in underdense plasmas. *Plasma Phys. Control. Fusion* **37**, 569 (1995).
- [35] A. Pukhov and J. Meyer-ter-Vehn, Relativistic magnetic self-channeling of light in near-critical plasma: three-dimensional particle-in-cell simulation. *Phys. Rev. Lett.* **76**, 3975 (1996).
- [36] T. W. Huang, C. T. Zhou, A. P. L. Robinson, B. Qiao, H. Zhang, S. Z. Wu, H. B. Zhuo, P. A. Norreys, and X. T. He, Mitigating the relativistic laser beam filamentation via an elliptical beam profile, *Phys. Rev. E* **92**, 053106 (2015).
- [37] V. I. Arnold, Lagrangian manifolds with singularities, asymptotic rays, and the open swallowtail. *Funct. Anal. its Appl.* **15**, 235 (1981).
- [38] R. G. Littlejohn, The van Vleck formula, Maslov theory, and phase space geometry. *J. Stat. Phys.* **68**, 7 (1992).
- [39] Y. A. Kravtsov, and Y. I. Orlov, *Caustics, Catastrophes and Wave Fields* (Springer, 1993).
- [40] S. C. Wilks, W. L. Krueer, M. Tabak, and A. B. Langdon, Absorption of ultra-intense laser pulses. *Phys. Rev. Lett.* **69**, 1383 (1992).